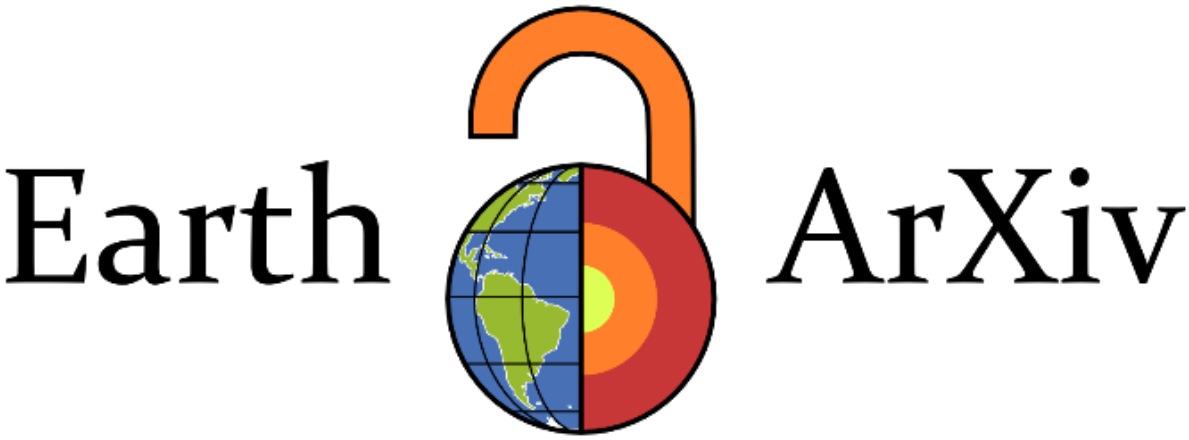

Mid-crustal Origin of Alkaline Magmas in the Arosa Zone: Evidence from Primary Analcime and Xenolith Interaction at the Rothplattenbach Complex (Germany)

Preprint, February 2026

Authors: Dr. Alfred Wassermann (a.wassermann@rmskempten.de), Matthias Hanke (hanke-matthias@t-online.de)

Keywords: Primary analcime, closed-system differentiation, Rothplattenbach, xenolith metasomatism, infiltration metasomatism, Rotkalk xenoliths, Rayleigh fractionation, thermodynamic geobarometry, alkaline magmatism, magma-carbonate interaction, European Cenozoic Rift System (ECRIS), meso-crustal emplacement, zeolite facies

---

Abstract

The petrogenetic evolution of the alkaline magmatic rocks of the Rothplattenbach Complex was investigated by X-ray diffraction phase analysis and crystallographic lattice-parameter determination. The study focuses on the identification of primary analcime occurring in paragenesis with Ca-rich plagioclase (An_{77}) and diopsidic clinopyroxene. Phase-equilibrium modelling indicates that magma evolution in a closed system through Rayleigh fractional crystallization resulted in chemical convergence toward an analcime-saturated melt composition. Thermodynamic stability constraints for analcime (P > 5 kbar, T < 660 °C) imply a subvolcanic origin from deep-crustal levels at 15–20 km depth, contradicting the previous interpretation of these rocks as near-surface pillow lavas.

Jurassic Rotkalk xenoliths record a zoned interaction ranging from isochemical recrystallization to marble (lattice expansion in calcite) to allochemical infiltration metasomatism. The formation of glauconite through reduction of iron oxides in the Rotkalk and the occurrence of thomsonite provide evidence for intense fluid-mediated magma–carbonate hybridization. Preservation of these high-pressure parageneses together with high amorphous contents indicates rapid release of the complex. These results demonstrate that water and alkali saturation are primary characteristics of Cenozoic rift-related magmatism.

Introduction:

Already Carl Wilhelm von Gümbel, in his *Geology of Bavaria* (1888), documented the prominent outcrops of so-called “Alpenmelaphyre” at the Rothplattenbach. Blocks of these rocks are transported downstream to the Ostrach valley. These rocks, traditionally referred to as “spilites” of the Arosa Zone, crop out along a trail branching westward from the service road to the Hirschalpe (at ~1300 m a.s.l.). Field observations reveal dark basaltic debris locally replacing light carbonate lithologies along the path, and spilites are exposed in road cuts and float blocks along the ridge between the two streams.

Zeolites infilling vesicles and fractures in the Rothplattenbach spilites have been repeatedly reported. Additional occurrences of these spilites have been described from the Wildbach valley near Hindelang, the Retterschwang valley at the foot of the Rotspitze, Birgsau, the Geißalpe below the Entschenkopf, and the Ränkertobel at the Riedberg Pass. The rounded bodies, commonly interpreted as pillow lavas, are associated with marbleized carbonate rocks. Jurassic carbonate units, including Aptychus-bearing limestones, occur as associated lithologies. According to Scholz, the carbonate components represent tectonically sheared strata (red Aptychus limestone). Zeolites in these rocks have so far been interpreted exclusively as secondary alteration products of the magmatic body. However, this interpretation fails to explain the pervasive occurrence of analcime, particularly within the groundmass of the spilites.

Experimental constraints on the pressure–temperature dependence of analcime formation were already provided by Peters et al. (1966). Pearce (1970) investigated the Crowsnest Formation (Canada), which is well known for inferred primary analcime. Kim and Burley (1971) examined analcime stability fields at pressures up to 5000 bar, demonstrating for the first time that primary analcime may occur as a phenocryst phase in volcanic rocks. Luhr and Kyser (1989) discussed criteria for primary analcime in Mexican lavas, and Karlsson and Clayton (1991) provided one of the key frameworks for distinguishing primary from secondary analcime in igneous rocks. More recent studies, including the Mecsek Mountains study (2025), document analcime crystals in carbonate ocelli, interpreted as transitional between primary magmatic and hydrothermal origin. In the investigated spilites, analcime occurs together with clinopyroxene and plagioclase as a constituent of the groundmass. This observation strongly argues against late, low-temperature hydrothermal zeolite formation and instead supports a primary magmatic or late-magmatic origin of analcime. This hypothesis, combined with a field excursion to the Rothplattenbach area in 2025, motivated a detailed phase-analytical investigation of spilite samples from the study area.

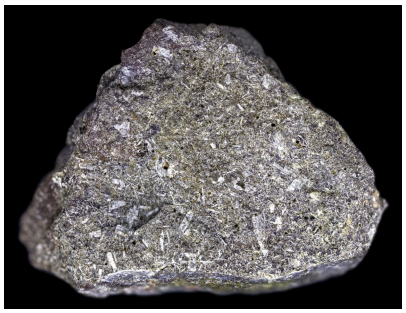

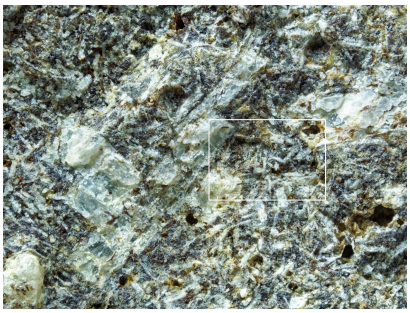

Figure 1:
Groundmass of the magmatic rock.
Plagioclase laths, clinopyroxenes, and analcime.
Object:
Width: 2.5 cm
Height: 1.5 cm
Depth: 0.6 cm
Image width: 3.2 cm
Enlargement:
Image width: 3.8 mm
Photos:
Matthias Hanke Collection

Primary analcime

Primary analcime has been reported mainly from silica-undersaturated alkaline magmatic rocks, such as basanites, phonotephrites, and certain lamprophyres. The question whether analcime is primary (crystallized from the melt) or secondary (formed by alteration of leucite) has been intensively debated in the literature. Chemical and mineralogical evidence supporting a primary origin has been presented in numerous studies.

Luhr and Kyser (1989) described analcime phenocrysts from the Colima volcanic complex (Mexico), where the groundmass consists of titanian salite (clinopyroxene), titanomagnetite, apatite,

and abundant volcanic glass. The Crowsnest Formation in Alberta, Canada (blairmorites) is famous for centimetre-sized analcime crystals, widely interpreted as primary (Pearce 1993). These rocks are extremely alkaline and contain analcime (up to 30–50 vol%), sanidine, melanite garnet, and aegirine–augite. Transitional varieties additionally contain plagioclase and diopside in the groundmass.

Analcime-bearing basanites from the Westerwald and the Hessian Depression commonly contain diopsidic augite and plagioclase (typically labradorite to bytownite, rarely pure anorthite) together with analcime in the groundmass. Tephritic analcimites from the České středohoří (Bohemian Massif) exhibit primary analcime in the groundmass associated with clinopyroxene and plagioclase laths. In the Colli Albani volcanic district (Italy), analcime-bearing rocks show parageneses with diopsidic clinopyroxene and very Ca-rich plagioclase (An contents > 80–90%). Analcime phonolites and tephritic rocks from the Kaiserstuhl volcanic complex also commonly contain primary analcime, particularly in transitional facies towards analcime-bearing basanites (limburgites). The Monzoni intrusive complex (Dolomites), although largely plutonic, displays a closely comparable mineral assemblage with fassaite (Ti-diopside), anorthite, and analcime.

In the Hegau volcanic field (e.g. Höwenegg, Stoffeln), analcime basanites and analcimites occur, and the groundmass typically contains diopsidic augite and plagioclase. Plagioclase laths commonly range from An_{70} to An_{85}. Extensive geochemical data demonstrate that these melts were extremely silica-undersaturated and water-rich, conditions favourable for primary analcime crystallization. Huckenholz (1977) provided major-element compositions (SiO_2, Al_2O_3, Na_2O, K_2O, etc.) indicating that analcime crystallized directly from the residual melt. Wilson and Downes (1991) presented geochemical data for Hegau alkaline basalts, including analcime-bearing varieties, in a European context.

In melilite–analcimites from the Urach–Kirchheim volcanic field (Swabian Alb), analcime commonly occurs as a primary groundmass phase. Although melilite is the dominant phase, less undersaturated varieties (“basalts”) also contain bytownitic plagioclase and diopside. Mäder (1983) reported detailed geochemical data for melilitites and analcimites, showing high Na_2O/K_2O ratios, which favour analcime over leucite formation. Analcime phonolites and tephritic dykes from the Kaiserstuhl also widely contain primary analcime, and plagioclase in mafic varieties reaches very high anorthite contents (up to An_{90}). The association of Ca-rich plagioclase with primary analcime is a strong indicator of high water vapour pressure (P_{H2O}). High melt water contents stabilize anorthite relative to albite and simultaneously allow analcime to crystallize directly from the melt. This combination is characteristic of differentiated magmas in continental rift settings of southern Germany.

Experimental studies by Roux and Hamilton (1976) in the $NaAlSi_3O_8$–$NaAlSiO_4$–H_2O system demonstrated that primary analcime is stable only within a narrow temperature window (<650 °C at P_{H2O} = 5 kbar). Thus, the melt must remain liquid at these low temperatures, requiring an appropriate eutectic composition. Experimental stability curves by Huckenholz (1977) and Roux and Hamilton (1976) are critical for the present study, as they define the P–T conditions under

which a melt of the composition observed in the Rothplattenbach magmatites can precipitate analcime.

Primary analcime exhibits a lower pressure limit and an upper temperature limit: below ~2.3 kbar analcime is unstable as a magmatic phase and decomposes to nepheline + albite + vapour. Even at high pressure, analcime melts incongruently at relatively low temperatures. At pressures above 5 kbar, the thermal stability limit is ~650–660 °C. Because basaltic melts (clinopyroxene + plagioclase) normally crystallize at temperatures >900 °C, primary analcime can only form if high water contents keep the residual melt liquid down to <650–660 °C.

The maximum stability temperature of analcime can be approximated by:

$$T = 600 + 15 \cdot (P - 2),$$

where T is in °C and P in kbar. At 5 kbar, this yields a maximum stability of ~645–655 °C, increasing to ~655–665 °C at 6 kbar. These constraints explain why primary analcime occurs in Hegau magmas under such conditions, whereas drier or more K-rich magmas (e.g. parts of the Kaiserstuhl) preferentially crystallize leucite or nepheline.

Magma evolution in a closed system

Sample 4 represents a rock body previously described as “spilite” and lacking xenoliths of Jurassic red limestone. From this sample, three subsamples (a–c) of the dark magmatic groundmass were collected and analysed by X-ray diffraction phase analysis.

Image 2: Sample 4

Photo: Matthias Hanke Collection

Dimensions:
Width (cm): 25
Height (cm): 24
Depth (cm): 11

All three analyses identified the zeolite analcime; natrolite was additionally detected in sample (b). Anorthite-rich plagioclase was present in all samples. Calcite detected in the samples was introduced during sample preparation from calcite veins and is therefore not considered a primary magmatic phase.

We interpret the system as closed, with no material influx into or outflux from the groundmass.

Bild 3:

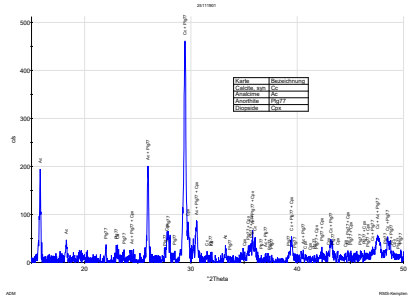

X-ray diffractogram of the matrix of sample 4.

The interferences of analcime (Ac), plagioclase (Plg77), and diopsidic clinopyroxene (Cpx) are clearly visible.

The detected calcite (Cc) did not originate from the matrix during preparation.

The groundmass of the investigated magmatic rock consists of plagioclase, clinopyroxene, analcime, and an amorphous component. The mean phase concentrations of all XRD analyses are:

Analcime	Natrolite	Plagioclase	Cpx
wt%	wt%	wt%	wt%
26,02	2,93	42,07	28,98
± 1,08	± 1,99	± 3,35	± 2,88

Initial magma composition

Based on the analytical data, the initial composition of the magma can be defined with high confidence. It corresponds to the blue-shaded field in the compositional triangle at T = 900–1100 °C and P > 5 kbar, consistent with a basaltic magma composition.

The composition of the plagioclase solid solution was determined from lattice parameters, in particular the unit-cell volume V_0. The mean unit-cell volume of the measurements is 669.308 Å^3, corresponding to an anorthite content of ~77 wt%. The calculated composition is $Ca_{0.77}Na_{0.23}Al_{1.77}Si_{2.23}O_8$.

The term “spilite” traditionally refers to hydrothermally altered (albitized) basalts. We use the term here only in a historical sense, as the measured plagioclase composition (An_{77}) clearly excludes a spilite sensu stricto (which would require An < 10).

The composition of clinopyroxene (Cpx) was also derived from lattice-parameter analyses. The detected clinopyroxene is a Na-, Fe-, and Al-bearing diopside with the composition $Ca_{0.955}Na_{0.045}Mg_{0.89}Fe_{0.133}Si_2O_6$.

Pressure–temperature constraints

The mineral assemblage provides independent constraints on pressure and temperature. The occurrence of primary analcime requires pressures > 5 kbar. In hydrous systems, the diopside solidus at 5 kbar is ~1100 °C, marking the onset of crystallization (Yoder, Roy, and Tuttle 1956). A plagioclase composition of An_{77} implies pressures > 6 kbar at 800 °C (Yoder, Steward, and Smith 1956).

To illustrate the chemistry of the relevant phases, the quaternary system nepheline–K-feldspar–anorthite–quartz is commonly used (after Yoder or Schairer). For better visualization of zeolite phases, we instead use the subtriangle $Na_2Al_2Si_2O_8$–Anorthite ($CaAl_2Si_2O_8$)–Quartz (SiO_2), where $Na_2Al_2Si_2O_8$ represents the carnegieite/nepheline component.

This triangle covers the entire compositional range from basaltic melts to strongly silica-undersaturated compositions. Analcime plots within this triangle (as a mixture of the Na component and quartz/H_2O), allowing graphical representation of melt evolution across the field.

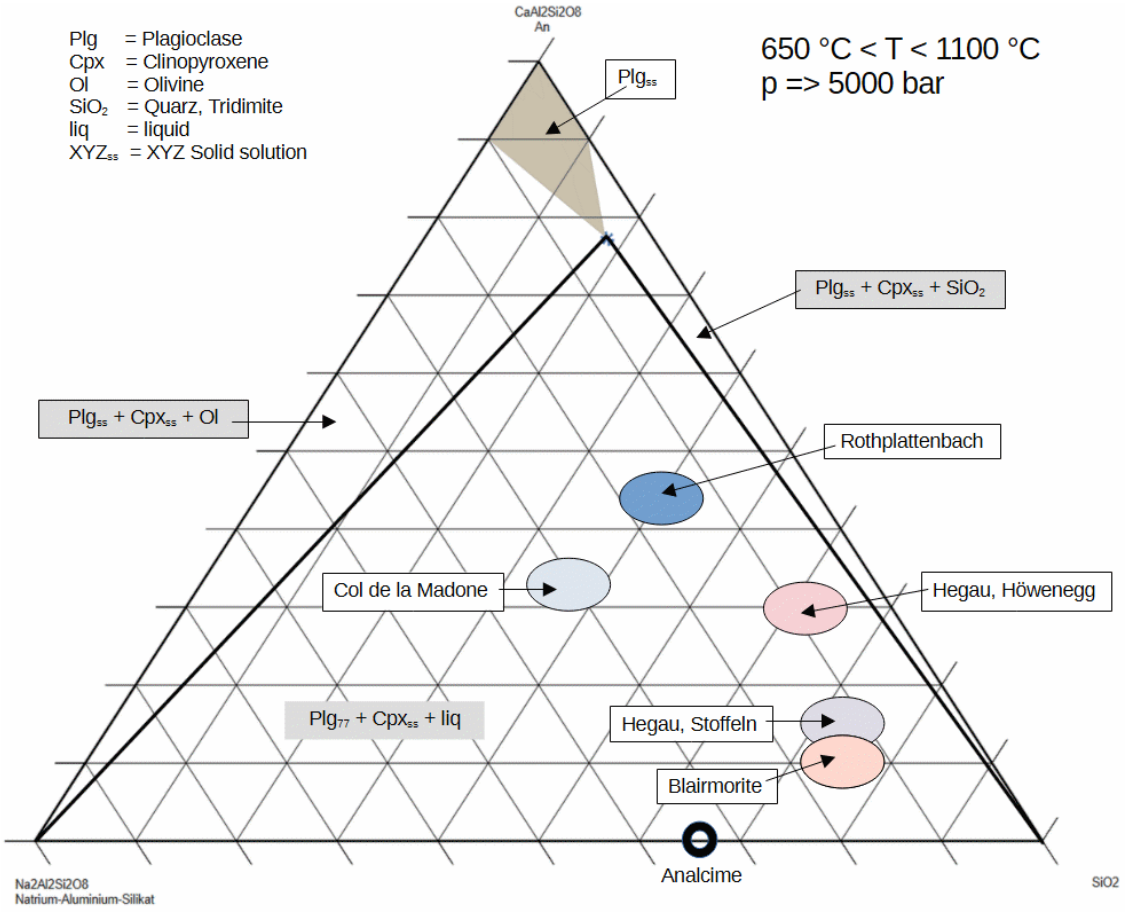

Figure 4: Compositional triangle 1.

Phase relations and fractional crystallization

At temperatures of 900–1100 °C and pressures > 5 kbar, the diagram shows the plagioclase solid-solution field and three phase fields. In the Na/Ca-rich domain, the assemblage Cpxss + Plgss + olivine is stable, whereas in the Ca/Si-rich domain the assemblage Cpx_{ss} + Plg_{ss} + SiO_2 occurs. Between these fields lies the large Cpx_{ss} + Plg_{ss} + liquid field; only this central field contains melt, whereas the two outer fields are fully crystalline.

Starting at ~1100 °C, decreasing temperature drives continuous cotectic crystallization. Components continuously crystallize from the melt, the melt fraction decreases, its composition evolves, and the Cpx/Plg_{ss} ratio adjusts accordingly. Melt compositional evolution can be modelled using Rayleigh fractional crystallization. To evolve from an average basaltic starting composition (Rothplattenbach) to the composition of analcime in a closed system, approximately 72–75% of the initial material must crystallize as clinopyroxene + plagioclase. This process results in residual enrichment of incompatible components (Na_2O and H_2O), such that the final residual melt (~25%) crystallizes as analcime.

The late-magmatic evolution towards analcime can thus be fully reconstructed in a phase-equilibrium framework. Between ~800 °C (P > 6 kbar; plagioclase formation) and the analcime stability limit (<660 °C), a cooling window of ~150 K exists. Within this interval, removal of Cpx

and An_{77} must drive the melt composition to converge precisely on the analcime composition at ~660 °C. Because pressure (>6 kbar) is well above the critical analcime threshold (~2.3 kbar), the only remaining variable controlling analcime saturation is the attainment of sufficient H_2O activity in the residual melt.

The compositional triangle includes not only the starting composition of the Rothplattenbach magma (blue field) but also initial magma compositions from Hegau–Höwenegg, Hegau–Stoffeln, blairmorites, and Col de la Madone. All plot within the same three-phase field. This indicates that primary analcime formation is not a local peculiarity of Rothplattenbach, Kaiserstuhl, or Hegau, but follows strict thermodynamic constraints. If a magma starts within the Cpx_{ss} + Plg_{ss} + liquid field, cotectic crystallization of clinopyroxene and plagioclase forces residual melts into the same compositional bottleneck, leading to chemical convergence toward analcime composition. The fact that diverse initial compositions—from intermediate blairmorites to mafic Hegau basanites—plot in the same field and all contain primary analcime strongly supports this hypothesis

Post-magmatic (autometasomatic) evolution in a closed system
With crystallization of primary analcime, the residual melt is exhausted. The rock is now fully solidified but remains mineralogically highly reactive; upon complete solidification, an aqueous fluid phase is released. These hot fluids circulate along grain boundaries.

During further ascent to shallower crustal levels, pressure decreases below the critical threshold of 5 kbar. The preservation of primary analcime in our samples requires either sufficiently rapid cooling to prevent decomposition into nepheline + albite + H_2O, or persistently high H_2O contents that expand the analcime stability field toward lower pressures.

Analcime is characterized by an open zeolitic framework, enabling extensive Na^+ exchange with other cations and further hydration processes.

The now-stable plagioclase (An_{77})–analcime conode defines the boundary between basaltic (olivine-bearing) and andesitic (quartz/tridymite-bearing) magma compositions.

Figure 5: Compositional triangle at 400–600 °C.

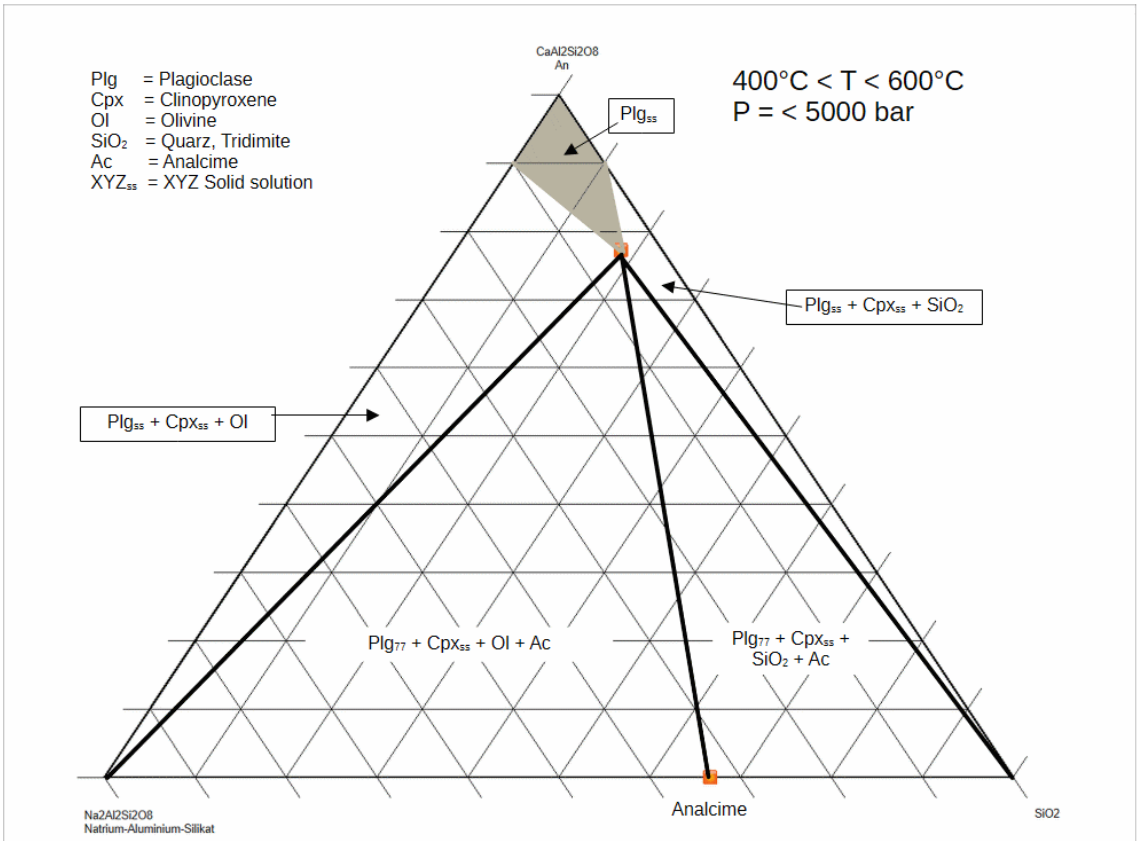

The parageneses shown in the compositional triangle at <600 °C and 5 kbar remain stable until further slow cooling releases fluids at ~400 °C, enabling thomsonite formation from plagioclase on the Na-rich side of the triangle:

Plgss + H_2O ⇌ Thomsonite + SiO_2
$NaAlSi_3O_8$ (Ab component) + 2 $CaAl_2Si_2O_8$ (An component) + 6 H_2O ⇌ $NaCa_2Al_5Si_5O_{20}{\cdot}6H_2O$ + 2 SiO_2

Figure 6: Compositional triangle at 250–400 °C.

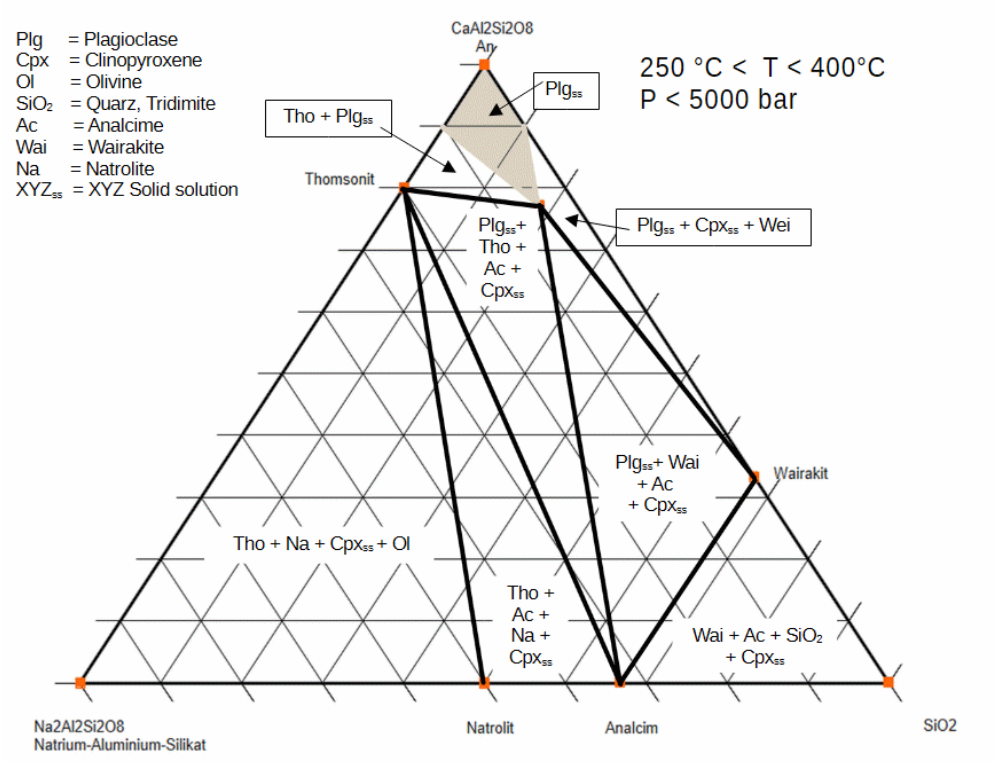

In a closed system, hydration of plagioclase to zeolites causes significant volume expansion, producing microfractures that enable fluid circulation and formation of late-stage phases.

On the SiO_2-rich side of the triangle, the liberated SiO_2 reacts just below 400 °C with the An component of plagioclase to form wairakite:

Plgss + SiO_2 + H_2O ⇌ Wairakite
$CaAl_2Si_2O_8$ (An component) + 2 SiO_2 + 2 H_2O ⇌ $CaAl_2Si_4O_{12}{\cdot}2H_2O$

The albite component of plagioclase forms natrolite (lower side of the triangle):

Plgss ⇌ Natrolite + SiO_2
2 $NaAlSi_3O_8$ ⇌ $Na_2Al_2Si_3O_{10}{\cdot}2H_2O$ + 3 SiO_2

Below 250 °C, wairakite hydrates to laumontite:
$Ca[Al_2Si_4O_{12}]{\cdot}2H_2O$ (wairakite) + 2 H_2O ⇌ $Ca[Al_2Si_4O_{12}]{\cdot}4H_2O$ (laumontite).

SiO_2 released during natrolite formation reacts with the An component of plagioclase and H_2O to form heulandite:
4 $CaAl_2Si_2O_8$ + 20 SiO_2 + 24 H_2O ⇌ $Ca_4Al_8Si_{28}O_{72}{\cdot}24H_2O$

Below 150 °C, laumontite hydrates to chabazite:
$Ca[Al_2Si_4O_{12}]{\cdot}4H_2O$ (laumontite) + 2 H_2O ⇌ $Ca[Al_2Si_4O_{12}]{\cdot}6H_2O$ (chabazite).

Figure 7: Compositional triangle <250 °C.

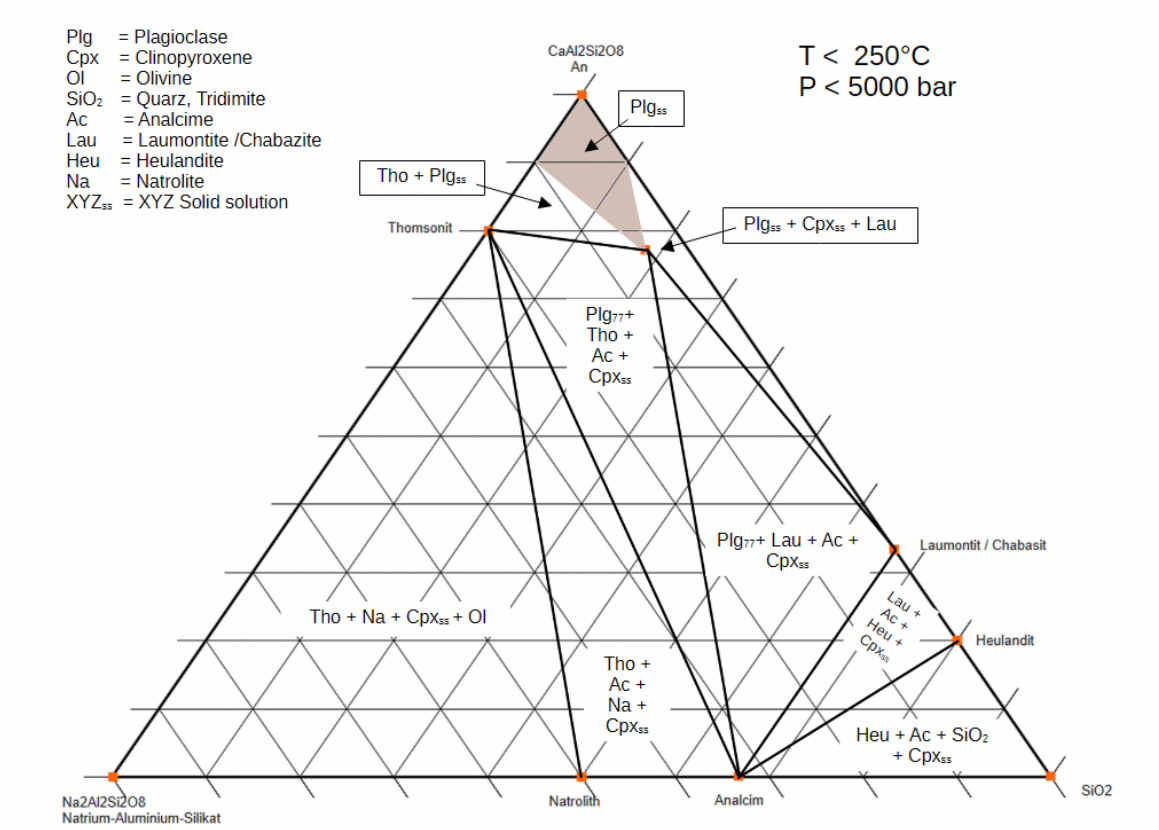

Interaction with xenoliths

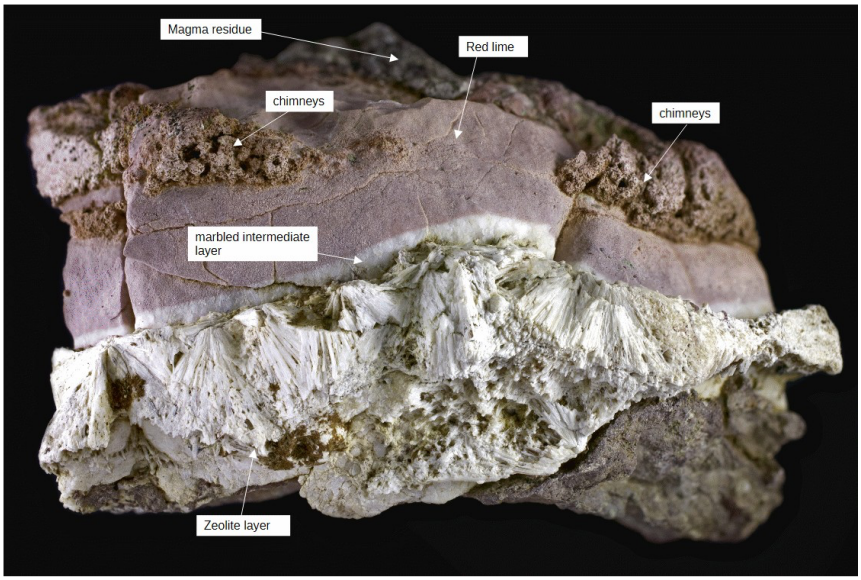

Figure 8: Sample 1

Dimensions:
Width (cm): 9
Height (cm): 6
Depth (cm): 4

Photo:
Matthias Hanke Collection

Figure 8 shows a sample from the Rothplattenbach area illustrating thermometamorphic reactions during contact between red Jurassic limestone and magma. The red limestone has previously been interpreted as entrained sedimentary blocks of Jurassic red limestone. XRD phase analysis of the limestone in this sample indicates a monomineralic calcite assemblage.

The lattice parameters of the limestone calcite are:
a_0 = 4.989 ± 0.001 Å, c_0 = 17.057 ± 0.015 Å
V_0 = 367.61 ± 1.6 Å³, c/a = 3.419

Downward in the image, the red limestone transitions into a relatively thin white intermediate layer, followed by a thick zeolite layer. The white intermediate layer also consists of pure calcite. Its diffractogram shows significantly lower counting statistics compared to the limestone, and crystallinity (1361 c/2θ) is much lower than that of the limestone (38659 c/2θ). The lattice parameters of this intermediate-layer calcite are:

a_0 = 4.989 ± 0.007 Å, c_0 = 17.12 ± 0.07 Å, V_0 = 369.18 ± 3.9 Å³, c/a = 3.431

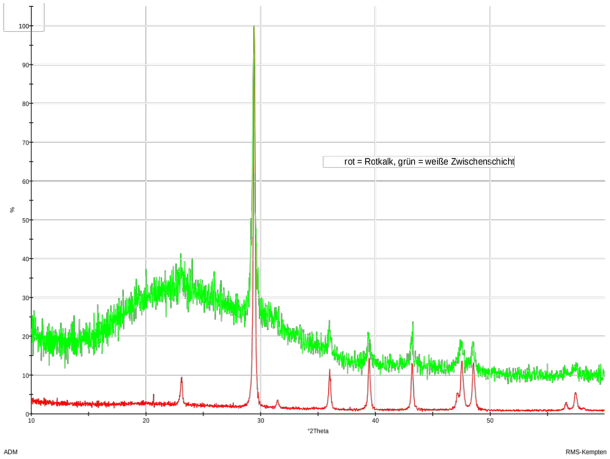

Figure 9: X-ray difractograms of the red limestone (red) and the marbled, white intermediate layer (green). The high proportion of amorphous material in the marbled intermediate layer is clearly visible.

The contact between Jurassic limestone and magma did not produce classical skarn mineralization but a narrow zone of isochemical recrystallization. Expansion of the calcite lattice in the intermediate layer (c_0 from 17.057 Å to 17.12 Å) accompanied by a collapse in crystallinity documents a rapid thermal pulse. During recrystallization, red-staining impurities were segregated and pure calcite recrystallized.

The absence of wollastonite supports the inference of high lithostatic pressure (>5 kbar) during magma evolution, suppressing calcite decarbonation. The overlying zeolite-rich layer marks the boundary where fluids from the H_2O-saturated magma interacted with recrystallized marble.

XRD analysis of the fibrous zeolite layer identified natrolite ($Na_2[Al_2Si_3O_{10}]\cdot 2H_2O$) and analcime ($Na[AlSi_2O_6]\cdot H_2O$). The contact zone with the limestone xenolith is therefore exceptional: a natrolite-rich layer (up to 85 wt%) with excellent crystallinity documents the action of a water-rich fluid phase at the contact. In contrast to the microcrystalline, thermally shocked calcite in the marble layer, sharply diffracting natrolite indicates undisturbed crystal growth in a stable hydrothermal halo. The white intermediate layer acted as a chemical barrier limiting mass transfer between the Ca-rich xenolith and Na-dominated magma, preserving the integrity of the closed system. This demonstrates extensive exsolution of water from the magma at the contact, corroborating our assumption of an H_2O-saturated melt at >5 kbar during primary analcime formation.

Fluid-escape structures and magmatic residues
Above the limestone in sample 1, chimney-like, upward-open structures embedded in magmatic material occur. These structures were initially interpreted as CO_2 fluid-escape conduits formed during thermal decomposition of calcite. Phase analysis, however, shows that these structures consist solely of analcime–natrolite aggregates. The absence of CaO or Ca-silicate phases refutes thermal decomposition of the limestone. Instead, these structures record directed ascent of magmatic fluids injected into the surrounding magmatic matrix due to the low permeability of the limestone xenolith. This confirms an H_2O-saturated system under high lithostatic pressure, where calcite stability was not exceeded.

Phase analysis of magmatic residues in sample 1 shows plagioclase, clinopyroxene, and zeolites (thomsonite and analcime). Calcite detected is likely preparation-related contamination from the underlying limestone. Notably, quartz is absent. The coexistence of primary clinopyroxene and plagioclase with analcime and thomsonite demonstrates that cooling and hydration followed the same closed-system petrogenetic pathway even in direct proximity to the xenolith. Local natrolite enrichment in chimney structures reflects mechanical segregation of fluid-rich residual phases, whereas the main magma preserved its mineralogical identity (Plg_{77}–analcime cotectic) up to the contact.

Progressive xenolith interaction (samples 2 and 3)

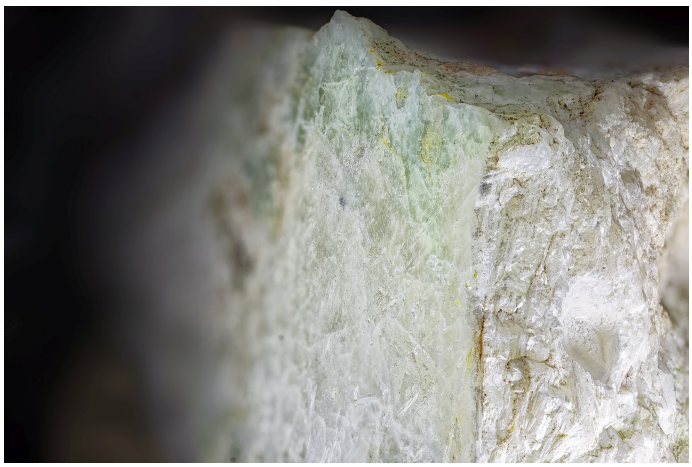

Image 10: Sample 2

Dimensions:
Width (cm): 14
Height (cm): 6.5
Depth (cm): 4

The sampling point on this sample can be seen in the right part of the image.

Photo: Matthias Hanke Collection

Sample 2 contains a polished white domain analysed by XRD. The diffractogram background between 15 and 40° 2θ indicates an amorphous component >20 wt%. In addition to calcite, thomsonite and natrolite were identified. In contrast to the purely physical marbling in sample 1, sample 2 documents intense chemical interaction. The >20 wt% amorphous fraction suggests local melting (palingenesis) or formation of a viscous silicate glass phase produced by reaction of magmatic fluids with the xenolith. Coexistence of thomsonite and natrolite indicates hybridization between magmatic Na and carbonate-derived Ca. The amorphous hump at 15–20° 2θ is consistent with a polymerized silicate structure typical of quenched, H_2O-rich residual melts or zeolitic precursors.

Figure 11: Sample 3

Dimensions:
Width (cm): 11
Height (cm): 12
Depth (cm): 8

The sampling point on this sample can be seen in the right part of the image.

Photo: Matthias Hanke Collection

Sample 3 also contains a limestone xenolith crosscut by white veins. Three subsamples were analysed. Phase analysis indicates >57 wt% amorphous material; crystalline phases include analcime (13 wt%), thomsonite (35 wt%), natrolite (25 wt%), wairakite (9 wt%), clinopyroxene (8 wt%), calcite (3 wt%), glauconite (5 wt%), and vermiculite (4 wt%).

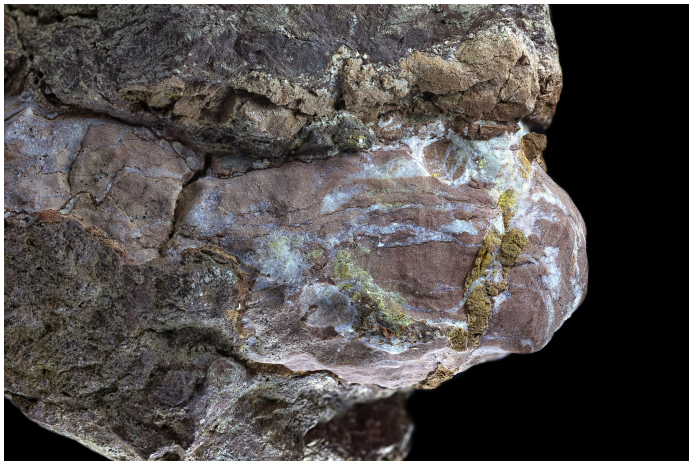

Figure 12: Sample 3, Sample a

Red limestone with white streaks.

The sampling point on this sample can be seen in the right part of the image.

Image width: 8.3 cm

Photo: Matthias Hanke Collection

Sample 3 documents advanced infiltration of the xenolith by magmatic fluids. The white veins consist of >57 wt% amorphous silicate, indicating rapid quenching of highly viscous, H_2O-saturated infiltrates. The analcime–natrolite–thomsonite assemblage again records hybridization between magmatic alkalis and carbonate-derived Ca.

The occurrence of glauconite represents a key reaction: Fe oxides in the limestone were reduced under hydrothermal conditions and incorporated, together with magmatic K, into sheet silicate structures. This marks the transition from purely thermal marbling to chemical replacement (metasomatism).

Endometamorphic zone and monomineralic analcime

Figure 13: Sample 3, Sample b

Red layer with a coarse structure

The sampling point is visible in the center.

Image width (cm): 4.1

Photo:

Matthias Hanke Collection

On the magmatic side of sample 3, a red, coarse-grained layer occurs at the limestone contact. Phase analysis shows dominantly analcime, with minor calcite likely from preparation contamination. This layer also contains an amorphous component and represents the endometamorphic zone. Dominance of analcime indicates persistence of magmatic alkaline chemistry to the immediate contact, whereas red pigmentation and coarse texture reflect intense hydrothermal interaction and Fe migration from the limestone, promoting analcime phenocryst growth.

Subsample (c) consists exclusively of analcime and shows a significant amorphous fraction.

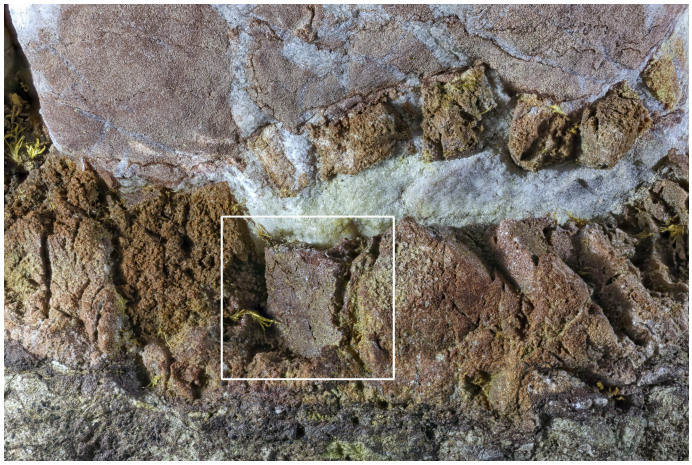

Figure 14: Sample 3, Sample c

Platy-formed analcime region

Image width (cm): 3.3

Photo: Matthias Hanke Collection

Discovery of monomineralic, platy analcime at the immediate contact marks the peak of hydrothermal activity and acted as a reservoir for subsequent limestone infiltration. Persistence of amorphous material throughout the contact zones indicates rapid cooling, preserving high-pressure magmatic phases (analcime) in a metastable state.

The platy morphology of analcime is not interpreted as a pseudomorph after plagioclase, as crystal dimensions exceed those of primary plagioclase laths in the host magma. Instead, this texture records directed crystal growth from a highly H_2O-saturated residual melt–fluid phase injected into the contact zone. The combination of monomineralic analcime growth and high amorphous fractions demonstrates the existence of a mobile analcime-normative melt–fluid phase during limestone interaction.

Synthesis
Samples 1–3 document a continuous increase in interaction intensity: from purely thermal buffering (isochemical marbling, sample 1), through incipient hybridization (sample 2), to complete metasomatic infiltration of the xenolith (sample 3). Persistence of analcime across all zones demonstrates dominance of an H_2O-saturated alkaline magmatic chemistry that remains stable even under extreme carbonate-contact conditions.

Analytical methods

Microscopic investigations were performed using reflected-light stereomicroscopes.

XRD analyses were conducted using a Panalytical PW 3710 diffractometer with a Cu anode operated at 40 kV and 40 mA. Data acquisition and crystallographic/phase analysis were performed using ADM-Suite V10 software, and the ICDD PDF-5 database was used for phase identification.

Geological Discussion and Conclusions

The phase-analytical investigations document a multistage magmatic evolution that transitions into pervasive autometasomatic (deuteric) alteration. The entire sequence developed under closed-system conditions, without requiring any external material input (e.g., seawater or groundwater). In

such a system, the water required for zeolite formation is derived primarily from the magma itself. Because water is not incorporated into early anhydrous phases (olivine, pyroxene), it becomes progressively enriched in the residual melt until water saturation is reached during cooling. The released magmatic fluids remain within the rock framework and react directly with the primary minerals (autohydration).

This process can be subdivided into the following stages:

Magmatic main stage (> 800 °C): Formation of the primary framework of clinopyroxene and anorthite-rich plagioclase.
Late-magmatic stage (< 660 °C): Crystallization of primary analcime from the water-saturated residual melt. At this stage, analcime, plagioclase, and clinopyroxene coexist stably.
Early hydrothermal stage (ca. 600 °C–200 °C): Formation of thomsonite and natrolite by reaction of magmatic fluids with the primary mineral assemblage.
Late hydrothermal stage (ca. 150 °C–50 °C): Very low-grade zeolite formation (zeolite facies) in the continuing closed system.

In parallel, hydrothermal processes may occur in externally open systems (fractures and veins), which also produce zeolite-facies assemblages. In these environments, natrolite and thomsonite dominate, whereas laumontite and heulandite occur in more SiO_2-rich domains.

Tectonic and Petrogenetic Implications
The coexistence of primary analcime and Upper Jurassic red limestone xenoliths serves as a precise barometer of regional tectonic conditions. The thermodynamic stability of analcime at 5–6 kbar, combined with the purely physical recrystallization of calcite (marbleization), requires that magma–xenolith interaction occurred at crustal depths of approximately 15–20 km. This implies a geodynamic process that transferred Upper Jurassic sediments to mid-crustal levels prior to intrusion by water-saturated alkaline magmas. The preservation of this high-pressure paragenesis, together with high amorphous contents (glass phases) in the contact zones, indicates subsequent rapid release, which kinetically inhibited subsolidus reactions and preserved metastable phases.

The present results contradict earlier interpretations of the Rothplattenbach magmatites as pillow lavas. Pillow lava formation in shallow marine environments is incompatible with the inferred pressure conditions (>5 kbar). Instead, the body represents a subvolcanic intrusive unit (sill or stock). The original magma originated in the upper mantle or lower crust and was transported rapidly to higher crustal levels. The rapid temperature decrease resulted from contact with significantly cooler crustal wall rocks in an active rift regime.

Interaction with Carbonate Xenoliths
A key aspect of the study is the interaction with carbonate xenoliths. Our data show:

1. During the initial stage, high ambient pressure suppressed decarbonation, preventing classical skarn formation (e.g., wollastonite).
2. With increasing hydration, infiltration metasomatism occurred. Magmatic, analcime-normative fluids penetrated the xenoliths and formed glauconite (via reduction of iron oxides in the red limestone) and hybrid zeolites (thomsonite).

3. The magma did not assimilate limestone on a large scale but displaced it metasomatically. This demonstrates that magma alkalinity is a primary mantle-source feature and not induced by crustal contamination.

Regional Context
Comparison with the Hegau, Kaiserstuhl, Blairmorites, Col de la Madone, and the Monzoni complex indicates that the formation of primary analcime follows a strict physicochemical laws. Magmas of the European Cenozoic Rift System (ECRIS) appear to ascend generally water-saturated from metasomatically modified mantle domains. The Rothplattenbach magmatite provides a compelling example of the transitional zone between deep-crustal crystallization and hydrothermal self-alteration.

Acknowledgements
We thank RMS Kempten for providing access to their XRD laboratory for the phase-analytical investigations. This research forms part of the study of Allgäu mineralogy and geology, initiated by the association *D'Allgeier Stoiklopfer e.V.* The authors also thank the anonymous reviewers for their critical and constructive evaluation of the manuscript.

Literatur:

Baier, J. (2020): *Das Urach-Kirchheimer Vulkangebiet der Schwäbischen Alb*. In: Der Aufschluss, Jahrgang 71, Ausgabe 4, S. 224–233.

Gottardi & Galli (1985): *The Zeolites*.

Gupta & Fyfe (1975): *Leucite-survival: The alteration to analcime*.
J. G. LIOU, CHRISTIAN DE CAPITANI & MARTIN FREY, Zeolite equilibria in the system CaAI2Si208 - NaAISi3O8 - SiO2 – H2O, *New Zealand Journal of Geology and Geophysics, 1991, Vol. 34:* 293-301

Geyer, M. & Gwinner, M. (2011): *Geologie von Baden-Württemberg*. 5. Auflage, Schweizerbart'sche Verlagsbuchhandlung.

Huth, T. & Junker, B. (2005): *Hegau – Geologische Kostbarkeiten*. (LGRB-Informationen zu den Deckenergüssen und Analcim-führenden Gesteinen am Stoffeln und Höwenegg).

Huckenholz, H. G. (1977): *Geology and Petrology of the Hegau Volcanic Province*.

Karlsson & Clayton (1991): *Analcime phenocrysts in igneous rocks: Primary or secondary?*

Kristmannsdóttir, H, Tómasson, J (1978): Zeolites zones in geothermal areas in Iceland In: L B Sand and F A Mumpton (eds), Natural Zeolites: Occurrence, Properties, Use, Pergamon, New York, 1978, pp 277-284

Kim & Burley (1971): *Analcime equilibria*.

Konya, Peter & Szakáll, Sándor. (2011): Occurrence, composition and paragenesis of the zeolites and associated minerals in the alkaline basalt of a maar-type volcano at Haláp Hill, Balaton Highland, Hungary. Mineralogical Magazine. 75. 10.1180/minmag.2011.075.6.2869.

Kushiro, I. (1969): *The system forsterite-diopside-silica with and without water at high pressures.* In: *American Journal of Science*, Vol. 267-A, S. 269–294.

Luhr & Kyser (1989): *Primary and secondary phlogopites and clinopyroxenes in alkaline lavas from the Colima Graben*.

Luhr, J. F. & Kyser, T. K. (1989): *Primary analcime in intermediate magmas from the Colima Volcanic Complex, Mexico.* In: Contributions to Mineralogy and Petrology, Volume 102, Issue 4, S. 420–439.

Mäder, U. (1983): *Die Geochemie der Tiefengesteins-Xenolithe des Uracher Vulkangebietes*. (Dissertation, ETH Zürich).

Mecsek Mountains Studie (2025): Neuere Untersuchungen in Ungarn zeigen Analcim-Kristalle in Kalk-Ocelli, die als Übergangsform zwischen primär-magmatisch und hydrothermal eingestuft werden.

Pearce (1970): *The Ti-variation in the basic rocks of the Crowsnest Formation*.

Pearce, T. H. (1993): *Analcime phenocrysts in igneous rocks: Primary or secondary?*. American Mineralogist.

Peters et al. (1966): *The stability of analcime and its neighbors*.

Karl August Reiser *„Über die Eruptivgesteine des Allgäu“, Dissertation* (1889), Deutsche Digitale Bibliothek – Digitalisierte Dissertation

Dieter Richter, *Allgäuer Alpen* (= *Sammlung Geologischer Führer*. Band 77). 3. Auflage. Gebrüder Borntraeger, 1984.

Dieter Richter, *Grundriß der Geologie der Alpen.* De Gruyter, 1974.

Roux, J. & Hamilton, D. L. (1976): *Primary analcite from igneous rocks*. In: *Journal of Petrology.*

Siegfried Schiemenz (1960), Fazies und Paläogeographie der subalpinen Molasse zwischen Bodensee und Isar , *Beihefte zum Geologischen Jahrbuch, Heft 38*, Niedersächsisches Landesamt für Bodenforschung, Hannover.

Schleicher, H. (1994): *The Urach-Kirchheim volcanic field*. In: Volcanism in the Upper Rhine Graben and its surroundings.

Scholz, H. (2016): *Bau und Werden der Allgäuer Landschaft*, 2016 E. Schweizerbart‘sche Verlagsbuchhandlung (Nägele u. Obermiller), Stuttgart, Germany

Scholz, H. [Hrsg.] (2023): *Wetzstein, Erz und Kohle. Nutzbare Gesteine, Minerale und andere Rohstoffe aus den Allgäuer Alpen, den westlichen Bayerischen Alpen und dem Alpenvorland.*– Mit insgesamt 29 Beiträgen, davon 18 von H. Scholz als Autor oder Mitautor, ca. 377 S.; Stuttgart (Schweizerbart-Verl.).

Spürgin, S. et al. (2019): *Zeolite-group minerals in phonolite-hosted deposits of the Kaiserstuhl Volcanic Complex*. American Mineralogist.

Wassermann, A. (1982): S*tabilitätsbeziehungen von Akermanit ($Ca_2MgSi_2O_7$) – Gehlenit ($Ca_2Al_2SiO_7$) Mischkristallen in Gegenwart einer binären H_2O – CO_2 Gasphase*. Dissertation, Ludwig-Maximilians Universität in München.

Wilson, M. & Downes, H. (1991): *Tertiary-Quaternary extension-related alkaline magmatism in Western and Central Europe*. In: *Journal of Petrology*, 32(4), S. 811–849.

Wimmenauer, W. (1962): *Die Phonolithe und Tinguaite des Kaiserstuhls*. Mitteilungen des Badischen Landesvereins für Naturkunde und Naturschutz, N.F. 8, S. 85–91. Zobodat PDF.

Wimmenauer, W. (2003): *Der Kaiserstuhl: Geologische Beschreibung eines Vulkangebirges*.

Wimmenauer, W. (1985): *Petrographie der magmatischen Gesteine*. (Enthält systematische Beschreibungen der Hegau-Vulkanite, inkl. Analcimiten)
.
Wimmenauer, W. (1962): *Die Phonolithe und Tinguaite des Kaiserstuhls*. Zobodat.

Wimmenauer, W. (2003): *Der Kaiserstuhl: Geologische Beschreibung eines Vulkangebirges*. (Detaillierte Diskussion der Primär-/Sekundär-Natur in der Matrix).

Yoder, H. S. & Tilley, C. E. (1962): *Origin of basalt magmas: An experimental study of natural and synthetic rock systems.* In: *Journal of Petrology*, 3(3), S. 342–532.